JAAS

Accepted Manuscript

Journal Name

ARTICLE

Rapid, direct determination of strontium in natural waters by laser-induced breakdown spectroscopy

Andrey M. Popov, [a] Anastasiya N. Drozdova, [b] Sergey M. Zaytsev, [a] Daria I. Biryukova, [a] Nikita B. Zorov, [a] and Timur A. Labutin*[a]

We report a LIBS technique of Sr determination in different types of natural waters, which provides sufficient sensitivity for strontium quantifying in marine studies, and for the safety control of drinking waters. The technique provides rapid measurements, not longer than 1 min per sample, without any preconcentration or dilution of waters. We demonstrated that the ionic line Sr II 407.77 nm was preferable for strontium quantification in natural waters than atomic line Sr I 460.73 nm, since the ratio between them equaled to ~30. One of the obstacles is a variability of total content of salts in waters from 0.01% to 5%. We found that the salinity had a strong influence on electron density (N_e): N_e grew up dramatically in case of low salinity (0 to 100 mg L^{-1}), and it did not change essentially for the salinity above 150 mg L^{-1}. At the same time, plasma temperature (~1.1×10^4 K) was independent from salinity. Since an increase of salinity suppressed ionic signal of strontium, the addition of NaCl as an ionization buffer diminishes considerably the matrix effects on analytical results. *LOD*s of Sr varied from 25 µg L^{-1} for pure or fresh waters to 200 µg L^{-1} for salty waters. We have shown that the suggested technique provided the accurate determination of strontium in samples of the Laptev Sea water and four types of mineral waters within the concentration range from 1 to 20 mg L^{-1}.

1. Introduction

Seawater Sr/Ca and Mg/Ca ratios are used to model global processes,[1] such as sea floor hydrothermal activity, formation of evaporites and dolomites, continental weathering, and changes in riverine fluxes, glaciation, and the dominance of aragonite vs. calcite precipitation from seawater etc., which are controlling the Sr, Mg, and Ca contents of seawater. The traditional approach to the marine research consists in a water sampling during expeditions, conservation and preservation of seawater and its subsequent analysis in the laboratory. At the final stage, such common methods of spectral analysis like flame photometry,[2] flame atomic absorption[3] and ICP-OES[4] are widely used. Currently, due to the development of technologies, manned submersibles and remotely operated vehicles can carry out *in situ* analysis of objects at great depths, providing an accurate geo-referenced chemical information. In this case only direct analytical methods can be used for real-time measurements[5] and informed decisions to be made. It is especially worth noting, that the content of magnesium and calcium in natural waters, varying from tens of mg L^{-1} in fresh water to ~several g L^{-1} in seawater and brines, is several orders of magnitude higher than that of strontium.

Since the average content of strontium in seawater is 7.9 mg L^{-1} and it is even less than in other natural waters,[6] poor sensitivity of direct analytical techniques may prevent from study of Sr/Ca ratio in the waters. It also should be noted, that strontium is isomorphic to calcium, and it is accumulated easily in a human bone tissue.[7] Therefore, its content in drinking water should not exceed 1.5-7 mg L^{-1} due to ecological or sanitary rules.[8,9] Significant variations of composition and salinity of natural waters (seawater, river water, mineral water *etc.*) is still a serious challenge for the direct analysis of aqueous samples. Thus, the samples are usually diluted in a hundred times to reduce the impact of salinity. For example, the ASTM Standard Test Method D 3352-03[10] for flame AAS Determination of Strontium in saline waters requires the dilution of seawater samples in 100-10000 times along with the adding of lanthanum as a releasing agent to minimize chemical interferences. On the other hand, Besson *et al.*[4] found that the 30-fold dilution was optimal for ICP-OES determination of main alkali and alkali-earth elements in seawater in terms of accuracy and reproducibility. Another approach is the pre-concentration[11] or electrochemical deposition[12,13] of the analyte from saline water with consequent analysis. There are a relatively few method for the direct determination of strontium in seawater. For example, ion chromatography[14] provides detection limit of 3 mg L^{-1}, which is too high for strontium determination. Obviously, the above methods cannot be placed in submersibles, although they may be used in onboard laboratory.

[a.] *Department of Chemistry, Lomonosov Moscow State University, Leninskie Gory, Moscow 119991, Russia, e-mail: timurla@laser.chem.msu.ru*
[b.] *P.P.Shirshov Institute of Oceanology, Russian Academy of Science, Nakhimovsky Avenue, Moscow 117997, Russia*
† Footnotes relating to the title and/or authors should appear here.

ARTICLE

Laser-Induced Breakdown Spectroscopy (LIBS) has been recently used for rapid remote analysis of various samples, including liquids.[15-18] This method is based on a focusing of a high-power laser radiation to generate laser plasma which emission is used for the qualitative and quantitative analysis. Moreover, LIBS instrument "ChemiCam" was deployed by submersible Hyper-Dolphin 3000 at depths more than 1000 m for *in situ* measurements[5] at the Iheya North field in the Okinawa. To our best knowledge, there are only few works on strontium determination by LIBS in liquids. Ng *et al.*[19] and Cahoon with Almirall[20] carried out strontium determination in water droplets (aerosols), generated by a special device, and they have achieved *LOD* of 20 and 1 mg L^{-1}, respectively. In the second case, the lower *LOD* was presumably achieved by the use of double-pulse excitation regime. In these works solutions with low salt content were analyzed, and it should be mentioned the difficulty of the use of the aerosol or droplet generator for high salinity water. Fichet *et al.*[21] have combined a jet technique with a gas stream (nitrogen) in ablation cell to produce the best analytical results. They reduced the *LOD* of strontium in aqueous solution to 0.34 mg L^{-1} with addition of Sc as internal standard. So, it seems reasonable to implement such a scheme for in-line analysis, but it is inconvenient for field analysis since formation of jet requires many additional parts and components (pumps, pipes, tank, *etc.*).

In this work, we focused on the direct determination of strontium in different types of natural water (fresh and sea water as well as mineral water), to provide sufficient sensitivity for quantifying Sr in marine studies, and for the safety control of drinking water. We studied the effect of salinity of natural waters on the parameters of laser plasma to determine the optimal experimental conditions in terms of sensitivity and minimal matrix effects.

2. Materials and methods

2.1. Experimental set-up

The experimental setup was described in details elsewhere in literature[22] and its scheme is presented in Fig. 1. Shortly, a beam of Nd:YAG laser at λ=532 nm (LOTIS, Belarus) passed through the high-efficiency mirrors (*M*) was focused with an achromatic doublet pair (*L*$_1$, *f*=150 mm) straight down onto a liquid surface. A glass cuvette (*GC*), having a wall thickness of 2.5 mm and a height of 40 mm, was half filled with liquid. We have mounted a thin quartz plate (*QP*) right after the *L*$_1$ to protect it from microdroplets. We reduced the laser energy behind *QP* from 130±2 mJ/pulse to 8.0±0.1 mJ/pulse by means of a set of neutral filters (*NF*) in order to prevent bubbles and sparks[18] in the volume of transparent liquid. In this case, we maintained a laser energy of high stability (*RSD*~1% at 8 mJ) in comparison with the change in the electrical power of pumping lamps (*RSD*>50% at 10 mJ). We have strictly controlled the laser energy over GC with a pyroelectric energy meter before the measurements of each solution. On the other hand, a focus of *L*$_1$ was displaced 1.5 mm below the
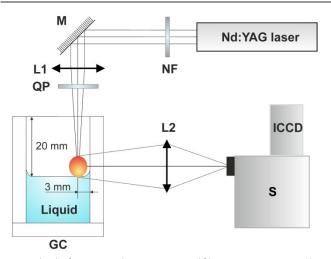

Fig. 1. A sketch of experimental setup: *NF* – neutral filters, *M* – mirrors, *L*$_1$, *L*$_2$ – lenses, *QP* – quartz plate, *GC* – glass cuvette, *ICCD* – CCD camera with an intensifier, *S* – Czerny-Turner spectrograph.

surface of a liquid to avoid a breakdown on the aerosol droplets. A stable transverse mode structure of the laser beam (TEM$_{01}$) as well as a stable laser energy provided a robust laser plasma. We have chosen the distance between the axis of the laser beam and the wall of *GC* equal to 3 mm for two reasons. First, the plasma had an unstable position on the meniscus of the liquid if the distance was less than 3 mm. Moreover, undesirable interactions of laser plume with the wall could be observed for shorter distances (<2 mm). Second, the emission spectrum of the plasma was weak for distances longer than 4-5 mm. Two-lens condenser (*L*$_2$, *f*=100 and 75 mm) projected an image of laser plasma onto the entrance slit (25 μm) of Czerny-Turner spectrograph (*S*, ISA Instruments, USA, resolving power 12 000 at 400 nm), equipped with ICCD camera (NanoSCAN, Russia). We accumulated signal from 20 consequent laser pulses for Sr signal measurements to enhance signal-to-noise ratio. Such arrangement is easy to use for either solids or liquids analysis, because *GC* can be quickly replaced by a solid sample without the changes of collection or focusing optics.

2.2. Chemicals and Materials

All the salts (NaCl, CaCl$_2$×2H$_2$O, MgSO$_4$×6H$_2$O, KCl, SrCl$_2$×6H$_2$0) used in this work were of at least ACS reagent grade (Sigma-Aldrich, USA). Strontium content in all reagents was less than 1 μg g^{-1} except for CaCl$_2$×2H$_2$O (Sr<0.01% wt). Deionized water with resistivity of 18.2 MΩ×cm was supplied from a three-stage purification system (Biospektr, Russia). Single channel mechanical pipettes of 100-1000 μL and 1-5 mL (Sartorius, Finland), 1 L, 250-, 100-, and 50 mL volumetric flasks were used to prepare solutions.

2.3. Preparation of solutions

Model solution imitated seawater was prepared in a 1 L flask by dissolving a salt mixture consisting of 27.197 g NaCl, 9.262 g MgSO$_4$×6H$_2$O, 1.553 g CaCl$_2$×2H$_2$O and 0.661 g KCl in deionized water. The composition of model solution and the averaged

ARTICLE

Table 1. Comparison between the composition of the prepared model solution (in mM) and the average composition of seawater (in mM)

Component	Model solution	Seawater
Na^+	466	468
K^+	8.9	10.2
Mg^{2+}	40.5	53
Ca^{2+}	10.5	10.3
SO_4^{2-}	40.5	28
Cl^-	496	546
Salinity, ‰	38.7	41

composition of seawater taken from Ref.6 (except for traces) are compared in Table 1. It should be noted that calcium sulfate did not precipitate in the model solution despite the fact that the ionic product, $c(Ca^{2+}) \times c(SO_4^{2-}) = 4.25 \times 10^{-4}$, was larger than the solubility product constant, $K_{sp}(CaSO_4) = 4.93 \times 10^{-5}$ at 25 °C.[23] High ionic strength of model solution (>1 M) raised the solubility of calcium sulfate by an order of magnitude as reported by Furby et al.[24] Therefore, we did not filtrate this solution before analytical measurements. Strontium content in the solution did not exceed 0.15 mg L^{-1} because there were strontium traces in a powder of calcium chloride dihydrate.

Stock solutions of Sr^{2+} and Na^+ were prepared by dissolving 346.5 mg of $SrCl_2 \times 6H_2O$ (100 mL flask) and 305.2 mg of NaCl (250 mL flask) in deionized water, respectively. Three sets of calibration solutions were prepared in 50 mL flasks: 0.8-255 mg L^{-1} of Sr in the model solution (No.1); 0.1-1140 mg L^{-1} of Sr in deionized water (No.2); and 0.5-201 mg L^{-1} of Sr and 150 mg L^{-1} of NaCl in deionized water (No.3). Their exact contents are given in Table 2. We placed a weighted powder of $SrCl_2 \times 6H_2O$

Table 2. Contents of calibration sets.

Compositions for blank solutions		
Set No.1	Set No.2	Set No.3
Deionized water Sr^{2+} <0.15 µg L^{-1} Na^+ 10.72 g L^{-1} K^+ 347 mg L^{-1} Mg^{2+} 972 mg L^{-1} Ca^{2+} 421 mg L^{-1} Cl^- 17.61 g L^{-1} SO_4^{2-} 3.89 g L^{-1}	Deionized water	Deionized water Na^+ 64.2 µg L^{-1}
Sr concentrations in sets, µg L^{-1}		
0.87	0.139	0.557
1.75	0.278	1.00
2.63	0.555	2.01
5.26	1.11	4.01
12.2	2.22	8.02
24.3	4.44	20.0
32.8	8.88	51.0
62.1	17.8	99.3
125	111	150.3
255	1140	201.3

inside a flask and then filled by model solution to the mark to avoid dilution in set No.1. Sets No.2 and No.3 were prepared by adding an appropriate amount of stock solutions to the flasks. High content of strontium in seawater (>300 mg L^{-1}) cannot be realized due to precipitating of $SrSO_4$ ($K_{sp}=3.44\times10^{-7}$ at 25 °C[23]).

2.4. Sampling of natural waters

A water sampling was performed at 7 complex stations during the August-September 2013 cruise of R/V Akademik Fedorov within the Nansen and Amundsen Basins Observational System (NABOS) program (see Table 3). Water samples were collected from the surface, nearbottom (usually two meters from the bottom), and intermediate horizons of the water column by the Niskin bottles mounted on a Rosette sampler. Water samples were filtered using precombusted at 430°C Whatman GF/F filters with pore size of 0.7 µm. The filtrate was collected into the acid-cleaned 20 mL glass vials, acidified by hydrochloric acid up to pH 2, and stored at the 3°C until further analysis.

Table 3. Seawater samples from the Laptev Sea and the St. Anna Trough collected in August-September 2013.

Sample No.	Station	Latitude, deg. N, min	Longitude, deg. E, min	Depth, m	Horizon, m
1	007	77°04.188	125°48.506	252	15
2					250
3	008	77°04.488	125°53.520	388	0
4					10
5					385
6	014	78°09.132	125°47.957	2450	0
7	015	78°24.091	125°45.343	2632	0
8	017	78°54.056	125°48.833	3022	0
9	059	77°42.232	126°52.446	1972	0
10	113	81°19.940	72°28.152	596	593

We have purchased in a supermarket four mineral waters (Borjomi, Yessentuki No.17, Yessentuki No.4, Novoterskay Healing Water) in 0.5 L glass bottles. Since all waters were carbonized, we removed the excess of CO_2 by an intensive long stirring before the measurements. Elemental composition of decarbonized mineral waters as well as seawater samples were analyzed by ICP-OES (ICAP-61 Thermo Jarrell Ash) with 50-fold dilution by deionized water. Their composition and the

Table 4. Composition (in mg L^{-1}) of mineral waters under investigation obtained by ICP-OES

Component	Borjomi	Yessentuki No.17	Yessentuki No.4	Novoterskay Healing Water
Na^+	1730±50	3100±80	2600±70	820±30
Mg^{2+}	33.3±1.5	60±3	25.0±0.6	59±3
K^+	26.7±1.0	21.3±0.5	14.7±0.4	58±3
Ca^{2+}	35.8±1.5	15.1±0.4	29.3±0.6	325±15
Sr^{2+}	6.2±0.3	3.0±0.2	4.9±0.3	16.3±0.4
Salinity, ‰	5.6	11.6	8.1	3.2

ARTICLE

Journal Name

estimation of total mineralization (i.e. salinity) are given in Table 4.

3. Results and Discussions

3.1. Analytical lines

A choice of analytical emission lines is a usual practice in spectral analysis to improve sensitivity. It is a question of vital importance for LIBS because the excitation conditions are strongly varied between LIBS plasmas.[25] Since both atomic (Sr I 460.73 nm[19]) and ionic (Sr II 421.55 nm[20,21]) lines were previously used for Sr determination in liquid jets or droplets by LIBS, we have compared the line intensities for two samples: the seawater No.5 (see Table 3) and a stock solution of $SrCl_2$. Plasma emitted light not longer than 5 μs due to low laser energy per pulse, therefore we have recorded plasma spectra with a delay of 0.5 μs and a gate of 2 μs to achieve maximal signal-to-noise ratios (*SNR*) and record the atomic and ionic lines under the same temporal conditions. The standard deviation of background within a spectral window without clear spectral features served as a noise. Since the line of Sr I 460.73 nm was invisible in case of seawater, only the LIBS spectra within the range around 406-423 nm are shown in Fig. 2. Broad line of H_δ I 410.17 nm belonging to Balmer series and the triplet of N I around 415 nm were clearly visible in seawater spectrum (curve 2 in Fig. 2) due to the high gain of ICCD (~250) in comparison with the stock solution of $SrCl_2$. Among two components of Sr II doublet (407 nm & 421 nm), we have selected the former line, since a degeneracy of its upper level was twice larger (4 *vs.* 2). It should be noted that *SNR* of ionic line at 407.77 nm was at least 30 times larger than *SNR* of the line of Sr I 460.73 nm in the case of stock solution of $SrCl_2$.
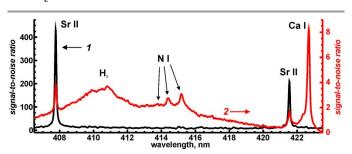

Fig. 2. LIBS spectra of two water samples: 1 (black trace, left axis) – a stock solution of $SrCl_2$, 2 (red right axis) - seawater No.5.

3.2. Plasma diagnostics

An explanation of such a difference between the intensities of atomic and ionic lines of strontium requires plasma diagnostics to be performed. We have estimated electron density of plasma by measurements of Stark broadening for line of H_α I 656.28 nm according to the equation given elsewhere in the literature.[26] Plasma temperature was calculated with the H_α and H_β lines of Balmer series by the two-lines method thoroughly described by Aragon and Aguilera.[27] Parameters of these lines are given in Table 5. Self-absorption of these

Table 5. Parameters of hydrogen and strontium lines

Line	λ, nm	ΣgA, $10^7 \times s^{-1}$	E_{upper}, eV
H_α	656.28	79.38	12.087
H_β	486.13	26.94	12.748
Sr II	407.77	56.40	3.039
Sr I	460.73	60.30	2.690

hydrogen lines are expected to be negligible because both transitions have the same lower level with high value of energy (~10.19 eV). A relatively small difference between energies of upper levels (~0.66 eV) can increase the relative error of temperature calculation according to our previous work.[28]

The averaged over 60 shots spectra of Sr stock solution are illustrated in Fig. 3. Experimental conditions were the same as those of Fig. 2. Because of the small Doppler width of the line (less than 0.05 nm at *T*=10 000 K), Lorentzian profile was the best fit for a profile of H_α (Fig. 3,a). We subtracted the instrumental width (~0.045 nm), measured by a He-Ne laser, from the Lorentzian width of the line to calculate electron density. The uncertainties for the Lorentzian width and the peak area were the errors of the fitting procedure of H_α line with the Origin Pro 8.1 software package. Since H_β line at 486 nm (Fig. 3,b) had an asymmetric dip within the line core, we have approximated an experimental profile of the line as a difference of two Lorentzian profiles. A considerable red shift (Δ=+0.14 nm) of a line center was a result of Stark broadening as reported earlier by Wiese *et al.*[29] Finally, the calculated plasma parameters were as follows: *T*=10 950±300 K and N_e=(2.9±0.1)×10^{17} cm^{-3}. Such a 'hot' plasma was unlike to 'cold' plasma in liquid jet,[30] but our estimation is close to the one
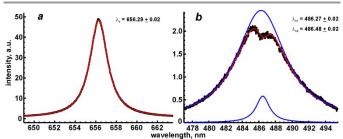

Fig. 3. LIBS spectra of a stock solution of $SrCl_2$ around hydrogen lines: H_α at 656 nm (*a*) and H_β at 486 nm (*b*). Black circles, red and blue curves correspond to experimental points, Lorentzian fits and two parts of H_β lines, respectively. Their central wavelengths are given in the legends.

obtained by Fabre *et al.*[31] for plasma torch on the surface of aqueous solutions (~11 500 K). The intensity ratio of Sr ionic to Sr atomic line (~32), calculated from Saha's equation, is close to experimentally observed one. For information, partition functions, retrieved from NIST Database,[32] are equal to 3.73 for Sr II and 8.64 for Sr I under the plasma conditions. Therefore, ionic strontium lines will be more preferable than atomic line in LIBS plasmas for sensitive determination of Sr.
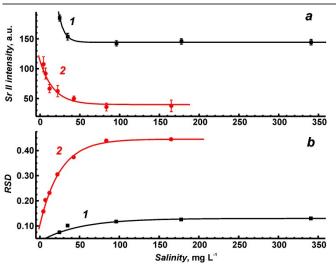
3.3. Salinity effect

Fig. 4. Salinity effects on the intensity (*a*) and *RSD* (*b*) of Sr II line at 407.77 nm obtained for two strontium concentrations: 8 mg L^{-1} (*1*) and 1 mg L^{-1} (*2*).

Fig. 5. Electron density of plasma as a function of the water salinity. A log-scaled plot is given in the inlets.

Since a salinity of natural waters is widely varied from <0.5 ‰ for river water to 5 % for brines,[6] we have investigated the intensity of Sr II line and its *RSD* as a function of salinity for two sets of solutions contained strontium of 1 and 8 mg L^{-1} (Fig. 4) and a variable content of NaCl. Data was averaged over 20 consecutive measurements to calculate *RSD*. One can easily see the suppression of Sr II line below 100 mg L^{-1}. Goueguel *et al*.[33] have recently observed an opposite effect in brines, when atomic lines of calcium or potassium increased simultaneously with the salinity. Such behavior of emission lines can be related to the shift of ionization equilibrium Na+Sr$^+ \leftrightarrow$ Sr+Na$^+$ from Sr$^+$ to Sr due to lower ionization potential of sodium. We have studied an influence of an easily-ionizable element (*EIE*) on the parameters of laser plasma to confirm this assumption. Electron density, calculated by the procedure above described, as a function of salinity is shown in Fig. 5. The main source of electrons under ablation of deionized water seems to be oxygen and hydrogen from water because their ionization potentials are very close to each other (~13.6 eV) and slightly lower than nitrogen (~14.5 eV). Obviously, the addition of a small quantity of *EIE*, such as Na (~5.2 eV) or Sr (~5.7 eV), should enhance ionization with increase of electron density. As one can see in Fig. 5, N_e increased dramatically up to salinities of 100 mg L^{-1} but then produced a plateau. Negligible variations of N_e were previously described by Goueguel *et al*.[33] for the brines. They believed that small variations in the electron density caused by matrix effects could not be detected experimentally. Taking into account a growth in the low salinity range, we suppose that two competing processes were responsible for such dependence. First, the ionization of Na and/or Sr atoms coming from extremely diluted solutions produces the large number of electrons. On the other hand, recombination of electrons and ions inside a plasma front restricts a further growth of N_e. It is important to note that both electron density and intensity of Sr II line changed slightly above salinity of ~100 mg L^{-1}. At the same time, plasma temperature was equal to 11 150±350 K for pure water, and this value is close for the one obtained for Sr stock
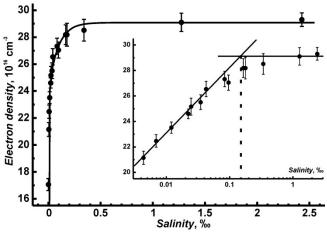
solution (10 950±300). Thus the plasma temperature does not differ significantly among the solutions, considering the uncertainties arising from the fitting procedure. Perhaps, either laser energy (8 mJ/pulse) fixed under experimental conditions or small variations of ablation threshold among a set of our aqueous solutions resulted in such an independence.

Since the salinity primarily influences the ionization equilibrium at low *EIE* content, we suggested their additive of 150 mg L^{-1} to achieve a stable ionization degree and, as a result, low sensitivity of analytical signal to variations in salinity of fresh waters. Such an additive is known in spectrochemical analysis as an *ionization buffer*,[34] which is added to increase the free-electron concentration in plasmas, and its application for stabilizing the degree of ionization is a usual practice for analysis by ICP-OES, flame AES or AAS. The dependencies of *RSD* (Fig. 4,b) on salinity are unexpected to be similar to a behavior of N_e (Fig. 5), i.e. the reproducibility is worsened up to a certain limit with an increase of salt content. A suppression of Sr II line by salinity (Fig. 4,a) is a possible reason for the worsening. Actually, the strontium signal for solutions containing 1 mg L^{-1} decreases in ~2.5 times (*curve 2* in Fig. 4,a), while its *RSD* increases in ~3.5 times (*curve 2* in Fig. 4,b). Another possible reason results from a visual observation of ablation process; so, the splashing of liquids was stronger for the saltier solutions. Anyway, it is important for analytical purposes to note that there were no considerable changes in both Sr II signal and its *RSD* above the salinity of 100 mg L^{-1} due to matrix effects. However, the reproducibility worsened, the signal suppressed and, as a result, the lower sensitivity for the determination of Sr in the saline waters are the costs to reduce matrix effects.

3.4. Analytical figures of merit

After several laser shots drops spread over the *GC* wall (see Fig. 1) due to a weak splashing of a liquid. As a result, the intensity of a radiation passed through the wall was systematically reduced in 5-10%. In spite of this value was within experimental *RSD*, we have gently shaken the cuvette after each 20 pulses needed for signal accumulation, to

ARTICLE

remove aerosol droplets from *GC* wall. Since this procedure was repeated 10 times for each sample to gather statistics, a duration of analytical measurements for a sample was about 1 minute (40 s for 200 shots at 5 Hz and 20 s for cuvette shaking). A peak area of strontium line after a baseline correction (the wing of hydrogen line H_δ) served as the analytical signal. We built linear calibration models for Sr determination within the concentration range of 0.5-25 mg L^{-1} for three sets of liquid samples described in the *Section 2.3*. The gain of ICCD in calibration measurements was set to 2^7 below 10 mg L^{-1} of Sr and to 2^5 at higher contents to avoid strong saturation of the signal. The parameters of calibration function $I_{Sr}=a+b\times c_{Sr}$ are listed in Table 6. *LOD*s were calculated according to 3σ-criterion. To estimate the noises accurately, we measured a blank sample which is specified in Table 2 for each set of calibration solutions. A feature is the same level of background intensity for all solutions due to broad H_δ line, which intensity is independent from the salinity. We calculated the blank intensity the same way as for strontium line in analyzed samples, assuming *RSD*s of the blank intensity over 10 pulses as noises. As one can see in Table 6, the largest slope of calibration curve (*b*) and the best sensitivity for Sr were observed for the non-saline solutions (set No.2). More than that, we observed a perfect calibration curve below 1.1 mg L^{-1} of Sr^{2+} (Fig. 6). In these terms, the evident advantage of ionic line is the reduction of *LOD* to 25 μg L^{-1} *vs.* the use of atomic line at 460.73 nm (20 mg L^{-1}, see Ref.19). More recently, Goueguel *et al.*[35] demonstrated that the *LOD* of strontium determination in water with the use of the resonance atomic line would be decreased to 2.89 mg L^{-1} by signal accumulation over 500 spectra. Poor sensitivity of the atomic line is related to the excitation conditions inside plasma, which do not promote sufficient intensity from strontium atoms. Simultaneously, the addition of *EIE* suppressed considerably the ionic line and, as a result, the slopes of calibration lines were decreased to virtually the same value for sets No.1 and No.3, as it can be expected due to the 'saturation' of N_e above 100 mg L^{-1} of salinity (see Fig. 5). It means the calibration curves become stable to the changes in salinity, while *LOD*s of strontium in saline solutions increased in 6-8 times.

Since the salinity had an effect on N_e, it certainly influenced the accuracy of Sr determination in different natural waters. We have compared the LIBS results of each set of calibration
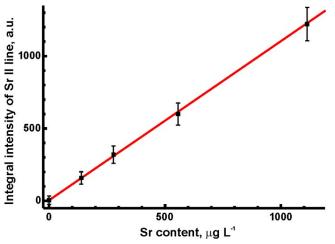

Fig. 6. Calibration curve obtained for calibration set No.2.

solutions with data from ICP-OES for accuracy evaluation. Accuracy plots are given in Fig. 7 as the correlation between data of two analytical methods. Blue and black points indicate seawaters and mineral waters, respectively. The parameters of linear function in the form of $c_{ICP-OES}=A+B\times c_{LIBS}$ are listed in Table 6. As one can expect, the large deviation of the line slope from unity, in the case of calibration solutions No.2 (see Fig. 7,c), results from the differences between the excitation conditions for solutions with small salts content. In other words, the calibration model constructed on the low-salt solutions (e.g. pure solution of SrCl$_2$ in deionized water) can not be considered as adequate one for analysis of natural waters with salt content larger than 1 g L^{-1} or 1‰, giving the strongly overestimated content of strontium. To avoid this, ionization buffer like a solution of NaCl should be added to the low-salt solutions. Such a way is the same for other emission methods (Flame-OES or ICP-OES). Actually, slopes *B* are close to unity, when we used the set No.1 (Fig. 7,a) and set No.3 (Fig. 7,b) of calibration solutions with content of salts more than 150 mg L^{-1}. Nevertheless, Sr contents obtained by all calibration models resulted in negative intercepts *A* of accuracy plot function, and, therefore, contents obtained by LIBS were slightly higher than for ICP-OES. Since the values of A are close to each other, we believe that the possible reason of non-zero intercept is the understated results of ICP-OES.

4. Conclusions

The experimental scheme proposed in the work allows the direct determination of strontium in different natural waters at the level of strontium abundance. The main feature of the scheme is the moderate reproducibility (*RSD*>5%) within the range of concentrations of 1-20 mg L^{-1} at low energy (8 mJ/pulse). We assume that the reason was a single transverse mode of a laser beam with a stable structure. The flexibility of the scheme allows easy adaptation of the conventional LIBS system to analysis of a small amount of liquid (less than 16 mL) in a conventional cuvette for spectrophotometry. Suggested experimental conditions provide rapid measurements (not

Table 6. Parameters for the linear calibration curves $I_{Sr}=a+b\times c_{Sr}$ obtained in three matrixes and the accuracy plots $c_{ICP-OES}=A+B\times c_{LIBS}$.

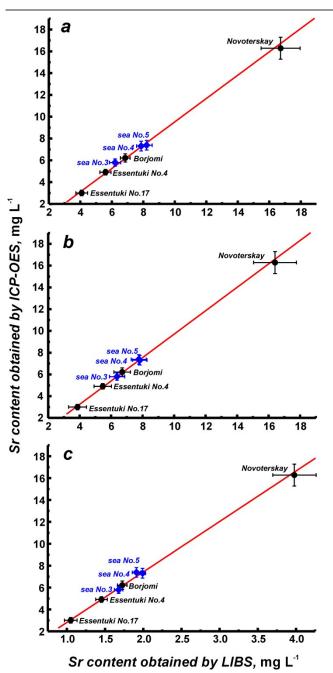| Calibration set	Set No.1 SrCl$_2$ + model seawater	Set No.2 SrCl$_2$ + deionized water	Set No.3 SrCl$_2$ + NaCl + deionized water
b	259±3	1104±2	267±3
R^2	0.999	0.999	0.998
LOD, μg L^{-1}	200	25	150
RSD at 1 mg L^{-1}	41.1	11.7	43.5
A, mg L^{-1}	-1.2±0.3	-1.8±0.2	-1.1±0.1
B	1.07±0.04	4.6±0.1	1.07±0.02

Fig. 7. Sr content determined by ICP-OES vs Sr content determined by LIBS for three sets of calibration solutions: (*a*) model sea waters, (*b*) Sr solutions in deionized water with an addition of 150 mg L^{-1} NaCl, and (*c*) Sr solutions in deionized water.

less than 500 mg L^{-1} or 0.5‰). The addition of NaCl (150 mg L^{-1} or more) as an ionization buffer diminishes considerably the salinity effect on analytical results. In spite of suppression of Sr II signal in salty waters, *LOD* of about 200 μg L^{-1} allowed the accurate determination of strontium in mineral waters and seawaters within the concentration range from 1 to 20 mg L^{-1}.

Acknowledgment

References:

1 S.J. Carpenter and K.C. Lohmann, Sr/Mg Ratios of Modern Marine Calcite: Empirical Indicators of Ocean Chemistry and Precipitation Rate, *Geochim. Cosmochim. Acta*, 1992, **56**, 1837.

2 T.J. Chow and T.G. Thompson, Flame Photometric Determination of Strontium in Sea Water, *Anal. Chem.*, 1955, **27**, 18.

3 E.E. Angino, G.K. Billings and N.R. Andersen, Observed Variations in the Strontium Concentration of Sea Water, *Chem. Geol.*, 1966, **1**, 145.

4 P. Besson, J. Degboe, B. Berge, V. Chavagnac, S. Fabre and G. Berger, Calcium, Na, K and Mg Concentrations in Seawater by Inductively Coupled Plasma-Atomic Emission Spectrometry: Applications to IAPSO Seawater Reference Material, Hydrothermal Fluids and Synthetic Seawater Solutions, *Geostand. Geoanal. Res.*, 2014, **38**, 355.

5 B. Thornton, T. Takahashi, T. Sato, T. Sakka, A. Tamura, A. Matsumoto, T. Nozaki, T. Ohki and K. Ohki, Development of a Deep-Sea Laser-Induced Breakdown Spectrometer for in situ Multi-Element Chemical Analysis, *Deep-Sea Res. Part I*, 2015, **95**, 20.

6 K.W. Bruland, R. Middag and M.C. Lohan, *Chapter 8.2 – Controls of Trace Metals in Seawater*, in: M.J. Mottl, H. Elderfield (Eds.) *Treatise on Geochemistry (Second Edition). Volume 8. The Oceans and Marine Geochemistry*, Elsevier, 2014, pp 19-51.

7 S.P. Nielsen, The biological role of strontium, *Bone*, 2004, **35**, 583.

longer than 1 min per sample) without any preconcentration or dilution of waters. The Sr II 407.77 nm spectral line was found to provide the best sensitivity (*LOD* 25-200 μg L^{-1}) which was explained by the influence of plasma properties on atomic-ionic equilibrium. Contrary to plasma temperature, electronic density is strongly affected by the total content of salts in solutions. Thus, N_e grows up dramatically in case of salinity varying between 0 to 100 mg L^{-1}, and it does not change essentially for the salinity above 150 mg L^{-1}. As a result, the ionic line is suppressed down to a certain constant value with the increase of salt content. This effect may appear to be the main obstacle to direct analysis of fresh waters (salinity

ARTICLE   Journal Name

8   Ecological risk assessment: freshwater screening benchmarks, available online: http://www.epa.gov/reg3hwmd/risk/eco/btag/sbv/fw/screenbench.htm. [2015, September 25]. US EPA.

9   Hygiene requirements and standards for drinking water SanPiN 2.1.4.1074-01 [in Russian]. Russian Ministry of Health: Moscow, 2001.

10   ASTM D 3352 – 03: Standard Test Method for Strontium Ion in Brackish Water, Seawater, and Brines.

11   H. Okamoto, Y. Okamoto, T. Hirokawa and A.R. Timerbaev, Trace ion analysis of sea water by capillary electrophoresis: determination of strontium and lithium pre-concentrated by transient isotachophoresis, *Analyst*, 2003, **128**, 1439.

12   A. Matsumoto, A. Tamura, R. Koda, K. Fukami, Y.H. Ogata, N. Nishi, B. Thornton and T. Sakka, On-Site Quantitative Elemental Analysis of Metal Ions in Aqueous Solutions by Underwater Laser-Induced Breakdown Spectroscopy Combined with Electrodeposition under Controlled Potential, *Anal. Chem.*, 2015, **87**, 1655.

13   G.D. O'Neil, M.E. Newton and J.V. Macpherson, Direct Identification and Analysis of Heavy Metals in Solution (Hg, Cu, Pb, Zn, Ni) by Use of in Situ Electrochemical X-ray Fluorescence, *Anal. Chem.*, 2015, **87**, 4933.

14   E.P. Nesterenko, P.N. Nesterenko, B. Paull, M. Meléndez and J.E. Corredor, Fast direct determination of strontium in seawater using high-performance chelation ion chromatography, *Microchem. J.*, 2013, **111**, 8.

15   D.A. Cremers, L.J. Radziemski, *Handbook of Laser-Induced Breakdown Spectroscopy,* 2nd ed., Wiley, 2013.

16   N.B. Zorov, A.M. Popov, S.M. Zaytsev and T.A. Labutin, Qualitative and quantitative analysis of environmental samples by laser-induced breakdown spectrometry, *Russ. Chem. Rev.*, 2015, **84**, 1021.

17   F.J. Fortes, J. Moros, P. Lucena, L.M. Cabalín and J.J. Laserna, Laser-Induced Breakdown Spectroscopy, *Anal. Chem.*, 2013, **85**, 640.

18   V. Lazic and S. Jovićević, Laser induced breakdown spectroscopy inside liquids: Processes and analytical aspects, *Spectrochim. Acta Part B*, 2014, **101**, 288.

19   K.C. Ng, N.L. Ayala, J.B. Simeonsson and J.D. Winefordner, Laser-induced plasma atomic emission spectrometry in liquid aerosols, *Anal. Chim. Acta*, 1992, **269**, 123.

20   E.M. Cahoon, J.R. Almirall, Quantitative Analysis of Liquids from Aerosols and Microdrops Using Laser Induced Breakdown Spectroscopy, *Anal. Chem.*, 2012, **84**, 2239.

21   P. Fichet, M. Tabarant, B. Salle and C. Gautier, Comparisons between LIBS and ICP/OES, *Anal. Bioanal. Chem.*, 2006, **385**, 338.

22   S.M. Zaytsev, A.M. Popov, N.B. Zorov and T.A. Labutin, Measurement system for high-sensitivity LIBS analysis using ICCD camera in LabVIEW environment, *J. Instrum.*, 2014, **9**, P06010.

23   *Section 5: Thermochemistry, Electrochemistry, and Solution Chemistry. Solubility Product Constants*, in: W.M. Haynes (Eds.), *CRC Handbook of Chemistry and Physics* (96th Edition)*, CRC Press, Internet Version, 2016.

24   E. Furby, E. Glueckauf and L.A. McDonald, The Solubility of Calcium Sulphate in Sodium Chloride and Sea Salt Solutions, *Desalination*, 1968, **4**, 264.

25   D.W. Hahn, N. Omenetto, Laser-Induced Breakdown Spectroscopy (LIBS), Part II: Review of Instrumental and Methodological Approaches to Material Analysis and Applications to Different Fields, *Appl. Spectrosc.*, 2012, **66**, 347.

26   R. Fantoni, S. Almaviva, L. Caneve, F. Colao, A. M. Popov and G. Maddaluno, Development of Calibration-Free Laser-Induced-Breakdown-Spectroscopy based techniques for deposited layers diagnostics on ITER-like tiles, *Spectrochim. Acta Part B*, 2013, **87**, 153.

27   C. Aragón and J.A. Aguilera, Characterization of laser induced plasmas by optical emission spectroscopy: A review of experiments and methods, *Spectrochim. Acta Part B*, 2008, **63**, 893.

28   T.A. Labutin, S.M. Zaytsev, A.M. Popov, I.V. Seliverstova, S.E. Bozhenko and N.B. Zorov, Comparison of the thermodynamic and correlation criteria for internal standard selection in laser-induced breakdown spectrometry, *Spectrochim. Acta Part B*, 2013, **87**, 57.

29   W.L. Wiese, D.E. Kelleher and D.R. Paquette, Detailed study of the stark broadening of balmer lines in a high-density plasma, *Phys. Rev. A*, 1972, **6**, 1132.

30   C.W. Ng, W.F. Ho and N.H. Cheung, Spectrochemical Analysis of Liquids Using Laser-Induced Plasma Emissions: Effects of Laser Wavelength on Plasma Properties, *Appl. Spectrosc.*, 1997, **51**, 976.

31   C. Fabre, M.-C. Boiron, J. Dubessy and A. Moissette, Determination of ions in individual fluid inclusions by laser ablation optical emission spectroscopy: development and applications to natural fluid inclusions, *J. Anal. At. Spectrom.*, 1999, **14**, 913.

32   A. Kramida, Yu. Ralchenko, J. Reader and NIST ASD Team (2015). NIST Atomic Spectra Database (ver. 5.2), Available online: http://physics.nist.gov/asd [2015, September 25]. National Institute of Standards and Technology, Gaithersburg, MD.

33   C. Goueguel, J.P. Singh, D.L. McIntyre, J. Jain and A.K. Karamalidis, Effect of Sodium Chloride Concentration on Elemental Analysis of Brines by Laser-Induced Breakdown Spectroscopy (LIBS), *Appl. Spectrosc.*, 2014, **68**, 213.

34   Compendium of Analytical Nomenclature: Orange Book of IUPAC. Definitive Rules; 1997. Part 10.3.4.3.5.

35   C. Goueguel, D.L. McIntyre, J. Jain, A.K. Karamalidis and C. Carson, Matrix effect of sodium compounds on the determination of metal ions in aqueous solutions by underwater laser-induced breakdown spectroscopy, *Appl. Opt.*, 2015, **54**, 6071.